AD_____

Award Number: W81XWH-10-1-0488

TITLE: Variations of Human DNA Polymerase Genes as Biomarkers of Prostate Cancer Progression

PRINCIPAL INVESTIGATOR: Nick Makridakis, Ph.D.

CONTRACTING ORGANIZATION: Tulane University, New Orleans, LA 70112

REPORT DATE: July 2013

TYPE OF REPORT: Final

PREPARED FOR: U.S. Army Medical Research and Materiel Command
Fort Detrick, Maryland 21702-5012

DISTRIBUTION STATEMENT: Approved for Public Release;
Distribution Unlimited

The views, opinions and/or findings contained in this report are those of the author(s) and should not be construed as an official Department of the Army position, policy or decision unless so designated by other documentation.

REPORT DOCUMENTATION PAGE

Form Approved
OMB No. 0704-0188

Public reporting burden for this collection of information is estimated to average 1 hour per response, including the time for reviewing instructions, searching existing data sources, gathering and maintaining the data needed, and completing and reviewing this collection of information. Send comments regarding this burden estimate or any other aspect of this collection of information, including suggestions for reducing this burden to Department of Defense, Washington Headquarters Services, Directorate for Information Operations and Reports (0704-0188), 1215 Jefferson Davis Highway, Suite 1204, Arlington, VA 22202-4302. Respondents should be aware that notwithstanding any other provision of law, no person shall be subject to any penalty for failing to comply with a collection of information if it does not display a currently valid OMB control number. **PLEASE DO NOT RETURN YOUR FORM TO THE ABOVE ADDRESS.**

1. REPORT DATE *(DD-MM-YYYY)*	2. REPORT TYPE	3. DATES COVERED *(From - To)*
July 2013	Final	15 June 2010–14 June 2013

4. TITLE AND SUBTITLE

Variations of Human DNA Polymerase Genes as Biomarkers of Prostate Cancer Progression

5a. CONTRACT NUMBER
W81XWH–10–1–0488

5b. GRANT NUMBER
W81XWH-10-1-0488

5c. PROGRAM ELEMENT NUMBER

6. AUTHOR(S)
Nick Makridakis

5d. PROJECT NUMBER

5e. TASK NUMBER

5f. WORK UNIT NUMBER

7. PERFORMING ORGANIZATION NAME(S) AND ADDRESS(ES)

Tulane University

New Orleans, Louisiana 70112–5406

8. PERFORMING ORGANIZATION REPORT NUMBER

9. SPONSORING / MONITORING AGENCY NAME(S) AND ADDRESS(ES)
U.S. Army Medical Research and Materiel Command
Fort Detrick, Maryland 21702 5012

10. SPONSOR/MONITOR'S ACRONYM(S)

11. SPONSOR/MONITOR'S REPORT NUMBER(S)

12. DISTRIBUTION / AVAILABILITY STATEMENT

Approved for public release; distribution unlimited

13. SUPPLEMENTARY NOTES

14. ABSTRACT
Human DNA polymerases beta, eta, and kappa are enzymes that function in repairing damaged DNA. We set out to identify and characterize the role of prostate tumor mutations in human genes POLB, POLH and POLK. We discovered missense mutations in all three polymerase genes. Biochemical analysis of the polymerase beta missense variations showed that all of these somatic mutations affect either polymerase activity, enzyme stability, DNA synthesis fidelity, or a novel endonuclease activity. We further showed that the Pol beta endonuclease activity prevents aneuploidy and genomic instability. Thus, frequent polymerase mutations may contribute to prostate cancer progression, through distinct enzymatic functions. These mutations are valuable as biomarkers of cancer progression.

15. SUBJECT TERMS
Biomarker discovery, cancer genetics

16. SECURITY CLASSIFICATION OF:			17. LIMITATION OF ABSTRACT	18. NUMBER OF PAGES	19a. NAME OF RESPONSIBLE PERSON
					USAMRMC
a. REPORT	**b. ABSTRACT**	**c. THIS PAGE**			**19b. TELEPHONE NUMBER** *(include area code)*
U	U	U	UU	38	

Table of Contents

INTRODUCTION

The early molecular events that lead to sporadic prostate cancer progression are largely unknown. Human DNA polymerases beta (Pol β) eta (Pol η), and kappa (Pol κ) are distributive error-prone enzymes that function in a relatively accurate manner when replicating damaged DNA. We set out to: (1) identify common somatic variants in the human pol beta, pol eta and pol kappa genes in prostate tumors. (2) Measure the frequency and distribution by tumor stage, tumor grade and patient age of each of the variants identified in Aim 1 in human prostate cancer tissues. (3) To determine the effect of the somatic variants identified in Aim 1 on polymerase function.

BODY

In Task 1, we set out to identify common somatic variants in the human POLB, POLK, and POLH genes in men suffering from prostate cancer. We thus sequenced the coding sequence of the POLB, POLK, and POLH genes for somatic mutations in 40 prostate cancer tissues, to test our hypothesis that prostate cancer tissue is commonly mutated in these genes. Briefly, we PCR amplified all exons using DNA isolated from microdissected prostate cancer tissue and then sequenced the PCR products bi-directionally on an ABI sequencer (detailed in Makridakis *et al*, 2009) or an HiSeq next-generation sequencer (ACGT Inc, Wheeling, IL). We have so far completed the POLB and POLK genes, and have also analyzed 7 exons of the POLH gene. We identified many somatic mutations in these samples, most of them missense. The POLH and most of POLB mutations have been reported (Makridakis *et al*, 2009). The somatic POLK mutations were reported in Makridakis *et al*, 2009, or on Table 1 of the Annual report of Year 2. We did not find any additional POLK or POLH mutations in year 3.

In an independent study, we are in the process of sequencing all DNA repair genes in the human genome (including POLB, POLK, and POLH) in 80 prostate tumors. We selected both low and high grade tumors that are matched for age, race/ ethnicity, and geographic location. These samples are of Caucasian American (50%), African American (40%) or Latino/ Hispanic origin (10%) and are from the Tulane/ LCRC biospecimen core. Following DNA isolation, we enriched our tumor and matched (i.e. from the same patient) normal samples for all DNA repair genes by using the SureSelect Target Enrichment method (Agilent Technologies, Santa Clara, CA). Briefly, genomic DNA samples were fragmented by sonication, linker ligated, and hybridized separately to the SureSelect DNA repair gene array. The RNA bait library (all exons of 129 targeted genes), was hybridized with the genomic DNA library. Unbound fragments were then washed away, and the DNA repair gene–enriched sequences were eluted and PCR-amplified (for 12-15 cycles) using the linker oligonucleotides that were ligated into the genomic DNA in the previous step. This target enriched DNA pool was then used in paired-end Next-generation DNA sequencing (NGS) on a HiSeq machine (Hussman Institute for Human Genomics). Bioinformatic analysis was performed at the Cancer Crusaders Bioinformatics Analysis core at Tulane Cancer Center, and it included mutation and gene-fusion analysis.

On the average, 70 % of reads mapped to our target genes, at > 200-fold coverage. Addition of tetramethylammonium chloride in the hybridization reactions resulted in improved coverage (>100-fold) of even GC-rich (>70% GC) sequences (data not shown). Although we only sequenced 20 tumors so far, a large subset of genes was somatically altered (showing significant loss of heterozygocity) across tumors derived from different individuals (data not shown). Furthermore, we identified somatic mutations in many DNA repair genes: XRCC1, CCNE1, ERCC2, MLH1, POLQ, OGG1, XPC, NFKB1, CDKN1A, POLB, E2F5, ABL1, MRE11A, ATM, CHEK1, CCND2, MDM2, POLE, BRCA2, ERCC5, CUL4A, and BRCA1. A partial list is shown on Figure 1. No novel mutations were found in POLK or POLH thus far. The somatic POLB mutations identified have not been reported before and are all missense: p.A42V, p.T93S, p.T93M, p.E172K, and p.T227I (Figure 1). The NGS approach can identify mutations that are present in <1% of the tumor cells in each tumor (unlike traditional sequencing), and is higher throughput and more cost effective (per base pair) compared to the genotyping approach proposed in Aim 2, so we plan on continuing this effort.

Gene ID	Gene Name	Mutations
BRCA1	Breast cancer 1, early onset	6(P440S), 6(E390K)
XRCC1	X-ray repair complementing defective repair in Chinese hamster cells 1	6(V44M)
ERCC2	excision repair cross-complementing rodent repair deficiency, complementation group 2	6(L91F)
CCNE1	Cyclin E1	6 (T395P)
MLH1	mutL homolog 1	6(R725S)
OGG1	8-oxoguanine DNA glycosylase	6(C255STOP)
NFKB1	nuclear factor of kappa light polypeptide gene enhancer in B-cells 1	6(R157STOP)
CDKN1A	cyclin-dependent kinase inhibitor 1A	6(P164L)
POLB	polymerase (DNA directed), beta	6(A42V), 6(T93S), 6(T93M), 6(E172K),

Figure 1: Partial list of somatic mutations of DNA repair/ cell cycle genes identified by NGS, in 20 prostate tumors.

Given the high number of somatic POL mutations identified by both conventional sequencing and NGS (including many missense), we decided to determine the effect of these variants on biochemical activity (Task 3) prior to establishing their frequency in sporadic prostate tumors (Task 2) (genotyping a high number of variants makes more sense when one knows that a significant proportion of these mutations are not mere passengers of cancer evolution; otherwise, we would rather focus on the functional variants).

We thus set out first to biochemically characterize the missense POLB variants. We initially focused on missense mutations because they have a higher chance of causing functional effects. Briefly, we reconstructed all missense Pol β mutations in an appropriate expression vector and then measured the effect of each mutation on enzyme activity, protein expression and fidelity of DNA synthesis *in vitro*, after purification of the respective overexpressed enzymes (detailed in An *et al*, 2011).

In vitro biochemical assays for both wild type (WT) and mutant POLB variants were performed on a single-gapped oligonucleotide substrate (the natural Pol β substrate). The experiments were performed at steady-state conditions for the enzyme, and the catalytic efficiency of each variant was determined, as a measure of enzyme activity. The results indicate that two of the Pol β variants significantly reduce catalytic efficiency (K27N and Triple mutant: P261L/ T292A/ I298T), while the remaining variants contain wild type activity (An *et al*, 2011, and Annual report Year 2).

The Triple Pol β mutant is interesting because it was homozygous in the tumor, and it abolishes polymerase

activity in vitro (An *et al*, 2011). The dramatic effect on Pol β activity is unexpected because the point mutations that comprise the triple mutant are not part of the active site (data not shown). In order to understand the effect of the individual point mutations on this clinically relevant variant, we recreated and biochemically analyzed all single and double mutants that comprise the triple mutant, using similar methods as in An *et al*, 2011. Biochemical assays for the variants using the gap-filling reaction (as above) showed that the dramatic loss of catalytic activity for the triple mutant is partially explained by its instability at 37 ^{o}C, and that the I298T mutation is responsible for this marked instability (Figure 1 of Annual report Year 2; An *et al*, in press, Appendix). Further biochemical characterization showed that the reduction in catalytic efficiency displayed by the Triple Pol β mutant is also due to a decrease in the apparent binding affinity for the dNTP substrate, which is due to the T292A mutation (Figure 2 of Annual report Year 2). We then proceeded to characterize the effect of these POLB variations on DNA synthesis fidelity using the same single-gapped oligonucleotide substrate (detailed in An *et al*, 2011). The results demonstrated that the triple mutant displays lower DNA synthesis fidelity for transversions *in vitro*, due to the T292A mutation (Figure 3 of Annual report Year 2; An *et al*, in press, Appendix). We conclude that distinct mutations of the Triple Pol β mutant are responsible for the loss of activity, lower fidelity, and instability observed: the I298T decreases enzyme stability, while the T292A decreases catalytic efficiency and DNA synthesis fidelity.

Fidelity measurements were also performed for the remaining POLB missense mutations identified (An *et al*, 2011). The data indicate that the majority of the POLB somatic mutations affect fidelity of DNA synthesis. Thus, two of the Pol β variants assayed (K27N and Triple mutant) reduce catalytic efficiency (An *et al*, 2011), while the remaining five missense mutations alter the fidelity of DNA synthesis (An *et al*, 2011). However, three of the somatic missense POLB mutations were anti-mutators (An *et al*, 2011), a finding that appears to be contrary to our model of increased mutagenesis generated in the tumors by mutations in error-prone polymerases. A potential explanation for this finding is the fact that DNA synthesis fidelity depends on sequence context (and we initially analyzed the mutants on a specific sequence context; An *et al*, 2011). Therefore, in order to better predict the mutagenic effect of these somatic POLB mutations, we utilized the Forward Mutation Assay (Bebenek *et al*, 2003). This assay relies on scoring errors produced by a DNA polymerase while filling a 407 nucleotide gap on the *lacZ* α gene, and thus can identify mutations in different sequence contexts (assay detailed in the Annual report for Year 2). Results of the forward mutagenesis assays demonstrated that the polymerase-proficient POLB variants E123K, E216K, and E232K, are indeed anti-mutators, regardless of mutation type (Figure 4 of the Annual report for Year 2). Thus we looked for an alternative explanation.

Pol β has recently been implicated in the early steps of meiotic recombination, which require either endo- or exo-nuclease activity (together with the topoisomerase SPO11; Kidane *et al*, 2010). We thus tested various Pol β variants for nuclease activity. Surprisingly, although the protein does not contain a known nuclease domain, pure human Pol β has endonuclease activity *in vitro,* cutting preferably recessed 3'-DNA ends, and even double-stranded DNA (a meiotic recombination hotspot and a human telomeric repeat; Figure 5 of the Annual report for Year 2). This endonuclease activity can be separated into a metal-dependent, prenicked-DNA stimulated activity and a metal-independent (but metal-stimulated) activity acting on intact DNA (Figure 5 of the Annual report for Year 2). In vivo, the initial cut may be performed by SPO11 (as in meiotic prophase), or

another endonuclease/ topoisomerase (in mitotic cells).

Pol β is known to translocate to telomeres during meiotic prophase following its role in meiotic recombination and homologous chromosome synapsis (Kidane *et al*, 2010). Modest (2-4 fold) Pol β overexpression induces aneuploidy, tumorigenesis, and telomere loses and fusions (Bergoglio *et al*, 2002; Fotiadou et al, 2004). Some of these extreme phenotypes may be related to the enzyme's novel nuclease activity.

We investigated the effect of the somatic missense POLB variations found in prostate tumors on endonuclease activity, using the recombination hotspot oligonucleotide. The results showed that the polymerase-proficient anti-mutator variants E123K, E216K and E232K specifically inactivated this activity (Figure 6 of the Annual report for Year 2). The T292A variant that affects DNA synthesis fidelity, also inactivates the endonuclease activity, while the K27N variant (which has reduced polymerase activity; An et al, 2011) has higher endonuclease activity (Figure 6 of the Annual report for Year 2). These data also show that the nuclease activity is specific to Pol β and not a contaminating E.coli nuclease activity (since a similar contaminating activity should be present in e.g. the E216K preparation). Moreover, *Pol β endonuclease activity is often inactivated in prostate tumors,* perhaps even more often than its polymerase activity. Thus *POLB* mutants found in various human cancers should be screened for their effect on endonuclease activity. Since POLB is mutated in 15-75% of tumors examined to date (Makridakis and Reichardt, 2012) this novel activity may be quite important.

Pol β endonuclease activity is weak *in vitro* (Figure 1), like other nucleases involved in DNA recombination (e.g. Mre11; Paull and Gellert, 2000). Further, the WT endonuclease activity against enzyme concentration curve is sigmoid (data not shown), suggesting complex kinetics and/ or cooperativity between subunits or multiple enzyme molecules. These two facts may help explaining the observation of a significant effect on nuclease activity by mutations that are not adjacent, based on the Pol β crystal structure (data not shown). Characterizing the Pol β endonuclease active site biochemically and structurally will be interesting and important and thus will be addressed in the future.

We questioned whether the weak Pol β endonuclease activity is important in mitotic cells *in vivo* (since the Pol β prostate cancer mutations are obviously independent of any role the Pol β nuclease may have in meiotic recombination). Unlike lower eukaryotes that depend solely on cohesin removal to separate sister chromatids in metaphase, higher eukaryotes also require topoisomerase II (Topo2), a *SPO11* homolog (Luo *et al* 2009). Thus DNA catenations may be a bigger problem in higher eukaryotes, inhibiting timely separation of the sister chromatids in metaphase. We hypothesized that Pol β endonuclease may assist Topo2 *in vivo* to separate sister chromatids. Thus we performed karyotype analysis of metaphase arrested (by colcemid) Pol β -/-, Pol β +/+ mouse embryonic fibroblast (MEF) cells (88Tag/ 92Tag), and also Pol β -/- MEF cells transfected with either WT or the nuclease-deficient E216K *POLB* mutant.

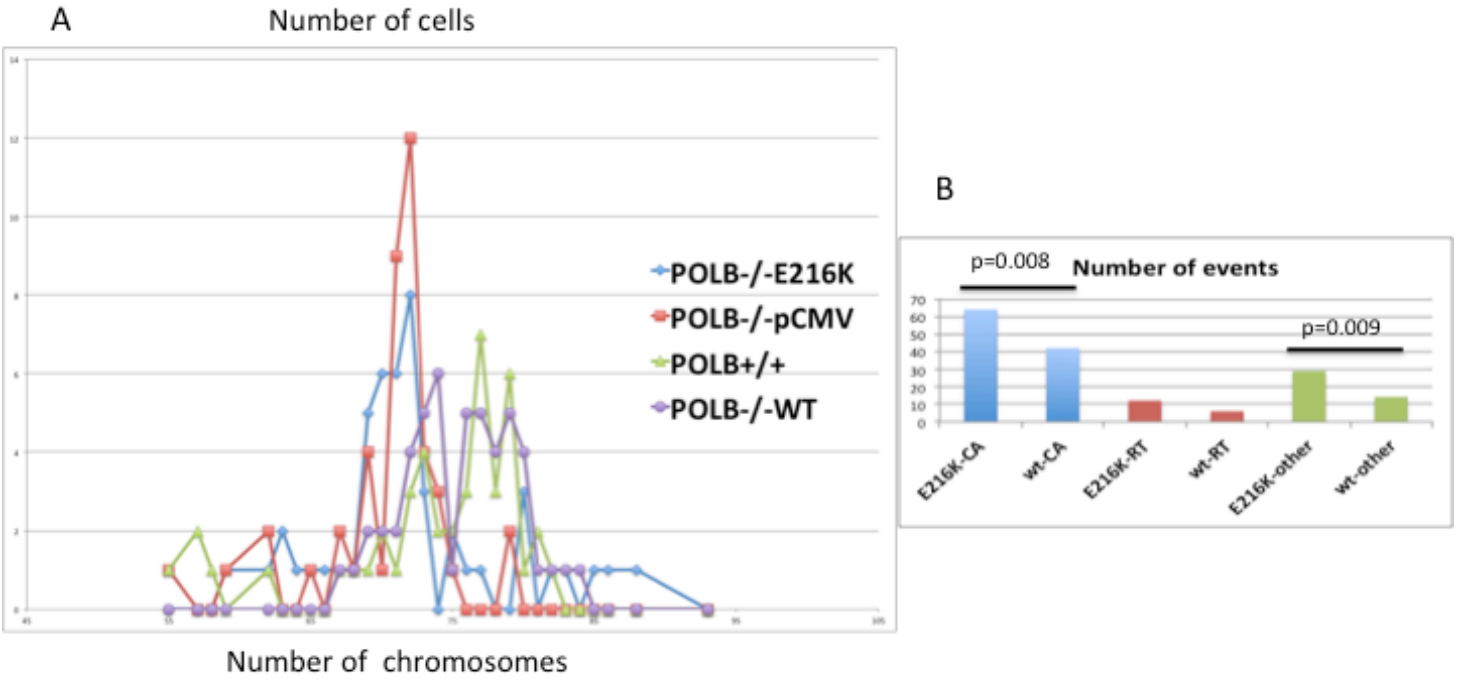

Figure 2: **Pol B nuclease prevents aneuploidy and genomic instability.**
Pol B-/- or PolB +/+ MEF cells were transfected with the indicated constructs (POLB E216K nuclease-deficient mutant, empty vector (pCMV), or WT POLB), and 48 hour post transfection, cells were arrested by colcemid, placed on slides, and stained by Giemsa for karyotype analysis. A. Analysis of chromosome number per cell (p=0.0004 for WT vs. E216K transfection). B. Analysis of chromosome defects. Key: CA: centromere associations; RT: Robertsonian translocations (centromere fusions); Other: chromosome breaks, fragments and fusions other than centromere fusions (eg. telomere to centromere or telomere to telomere). wt in panel B indicates mouse PolB -/- cells transfected with human WT POLB.

Both Pol β -/- and Pol β +/+ MEF cells are usually tetraploid, because they are transformed by SV40 large T antigen, but Pol β -/- cells are often aneuploid (Figure 2A). Karyotype analysis showed that transfection of the polymerase proficient (An *et al*, 2011) nuclease-deficient E216K mutant cannot correct the aneuploidy seen in Pol β -/- MEF cells (Figure 2A), while WT Pol β does (p=0.0004), suggesting that *the Pol β endonuclease activity prevents aneuploidy in vivo*. Western blots showed that the E216K and WT transfections expressed equal amounts of Pol β, indicating that the observed aneuploidy is not a result of different enzyme levels (data not shown). In addition, E216K transfected Pol β -/- cells display significantly more centromere associations and chromosome breaks/ fragments ("other" events; Figure 2B) compared to WT-transfected Pol β -/- cells, suggesting that these defects may lead to aneuploidy in the absence of Pol β nuclease. We conclude that *nuclease-deficient POLB mutations found in prostate tumors may contribute to cancer progression by increasing aneuploidy*. Aneuploidy is considered an early event in carcinogenesis, so these POLB mutations may be quite important for prostate cancer progression.

For Task 3, we also started to biochemically analyze the somatic missense POLK variants identified in prostate tumors (Table 1 of the Annual report of Year 2). Specifically, the E29K, F155S and G154E POLK mutants were generated on *E.coli* expression vectors using site directed mutagenesis and purified after bacterial expression. DNA polymerase assays were carried out with a DNA substrate containing an AP (apurine) site and purified human Pol κ (WT or E29K). After incubation at 37°C for 10 min, reactions were denatured, resolved on a 15% PAGE, and visualized by autoradiography. Kinetic analysis shows that the somatic E29K *POLK* mutation significantly decreases AP-site bypass efficiency (Figure 3). This mutation was found in an early-

onset tumor. These data support our hypothesis that functional error prone polymerase gene mutations may play an important role in prostate tumor progression.

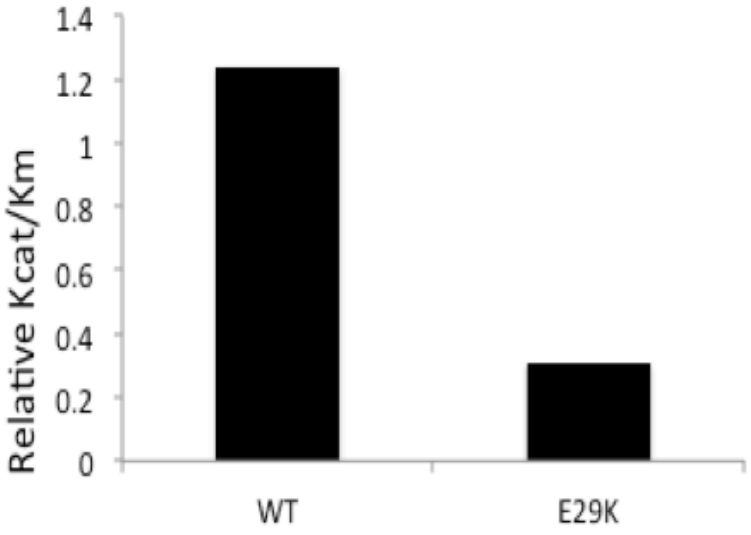

Figure 3: **Somatic POLK E29K mutation reduces catalytic efficiency**. WT and E29K *POLK* mutant variants were assayed for polymerase activity on an apurine site- containing DNA substrate, and the catalytic efficiency (*k*cat/*Km*,dATP) was determined, in triplicate assays. The average values are displayed.

Statistical analysis demonstrated that with the exception of one POLK missense mutant, all missense POL gene mutations were found in Caucasian patients. This is significant, because 40% of the patients examined were African American. Thus we conclude that POLB/ POLK genes are not commonly somatically mutated in African Americans. The distribution of the POL gene mutations by patient age was similar to the overall sample distribution (data not shown). However, The POL gene mutation distribution by tumor stage indicated that POLB missense mutations were most commonly found in Stage 3 tumors (Figure 4). Thus, *missense POLB mutations may be important biomarkers of advanced prostate cancer*. In addition, four missense somatic POLK mutations (E29K, G154E, T205I and L442F), the G259R POLH missense mutation, and four somatic POLB mutations (E216K, M236L, the Triple mutant and an AG splice junction mutation), were found in early onset prostate tumors. *These POL gene somatic mutations may be good biomarkers of presymptomatic disease*.

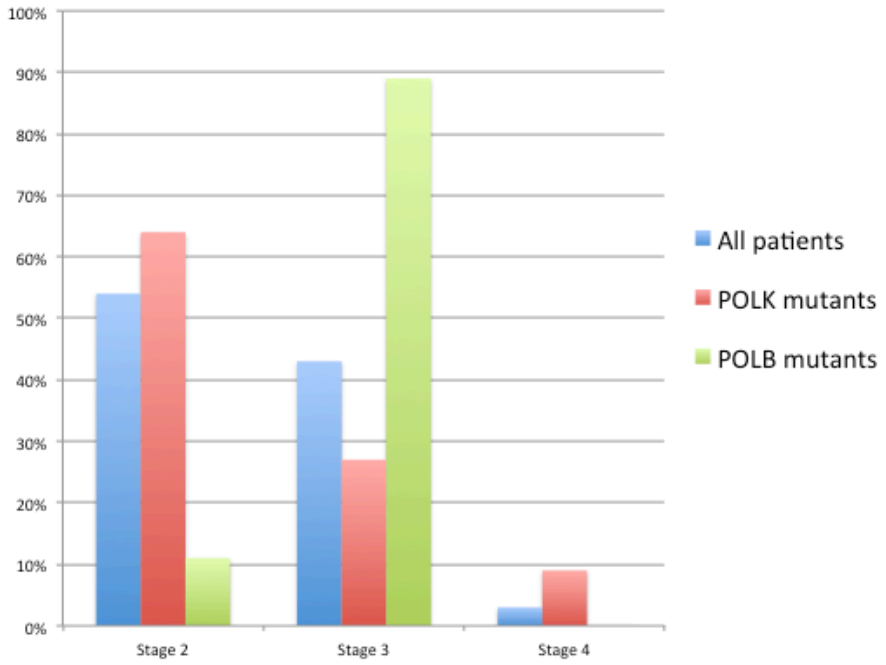

Figure 4. **Distribution of Pol gene mutations by tumor stage.**

KEY RESEARCH ACCOMPLISHMENTS

- Identification of frequent somatic variants of the human POLB, POLH and POLK genes in prostate cancer tissue
- Characterization of the biochemical effects of all missense POLB prostate cancer tissue variations identified (including all single and double mutant combinations of the Triple mutant), and some POLK mutants
- Discovery of a novel enzymatic activity of human Pol β (double-stranded DNA endonuclease), which prevents aneuploidy and genomic instability, and is inactivated in prostate tumors
- Characterization of important biomarkers of advanced prostate cancer and early-onset tumors.

REPORTABLE OUTCOMES

Manuscripts

An C, Chen D., and Makridakis NM. Systematic Biochemical Analysis of Somatic Missense Mutations in DNA Polymerase β Found In Prostate Cancer Reveal Alteration of Enzymatic Function. Hum Mutat, 32: 415-423, 2011.

Makridakis NM , and Reichardt JKV. Translesion DNA Polymerases And Cancer. Frontiers in Genetics, 3: e00174, 2012. doi=10.3389/fgene.2012.00174.

An C, Beard WA, Chen D, Wilson SA, and Makridakis NM. Understanding the loss of function in a triple missense mutant of DNA polymerase β found in prostate cancer, (*In Press*), 2013

Abstracts

Chen D, Mukhopadhyay S, Yadav S, and Makridakis N. Polymerase genes, genomic instability and Prostate Cancer, *LCRC Annual Scientific Retreat*, *Xavier University*, New Orleans, LA. 2011.

Yadav S and Makridakis N. DNA polymerase activity and translesion DNA synthesis by human polymerase kappa mutants. *Health Sciences Research Day,* Tulane University, New Orleans, LA, 2011.

Chen D, Lecompt K, Pursell Z, and Nick Makridakis. Somatic polymerase beta mutations found in prostate cancer differentiate between polymerase and endonuclease activity. *LCRC Annual Scientific Retreat*, *Xavier University*, New Orleans, LA. 2012.

Yadav S, Mukhopadhyay S, Chen D, Bhasin N and Makridakis N. Targeted Next-Generation Sequencing in DNA Repair Genes in Prostate Cancers. *LCRC Annual Scientific Retreat*, *Xavier University*, New Orleans, LA. 2012.

Chen D, Lecompt K, Pursell Z, and Nick Makridakis. Systematic analysis of the DNA synthesis fidelity of somatic mutations of polymerase beta found in prostate cancer. *Proc. Am. Assoc. Cancer Res,* A3121, Chicago, IL, 2012.

Mukhopadhyay S, and N. Makridakis. The human DNA polymerase kappa gene is frequently mutated in prostate cancer. *Health Sciences Research Day, Tulane University,* New Orleans, LA, 2012.

Carron E, Chen D, and Makridakis N. DNA Polymerase β Deficient Cells Are Hypersensitive to Camptothecin. *Biomedical Sciences Retreat 2012,* La. Universities Marine Consortium, Chauvin, LA, 2012.

Yadav S and Makridakis N. Targeted Next-Generation Sequencing in DNA repair genes in prostate tumors *Proc. Am. Assoc. Cancer Res,* A4228, Washington, DC, 2013.

Chen D, Carron E, and Makridakis N. Human DNA polymerase beta endonuclease activity prevents aneuploidy and Robertsonian translocations. *LCRC Annual Scientific Retreat*, *LCRC*, New Orleans, LA, 2013.

Yadav S and Makridakis N. Optimization of depth coverage of GC-rich exon 1 in DNA repair genes for next generation sequencing. *LCRC Annual Scientific Retreat*, *LCRC*, New Orleans, LA. 2013.

Presentations

Makridakis N. DNA repair genes, genomic instability and Prostate Cancer, School of Medicine, University of Athens, Athens, Greece, 07/10

Makridakis N. Error-prone polymerase mutations and prostate cancer progression, COBRE/Cancer Genetics group seminar, Tulane University, New Orleans, LA, 08/10

Makridakis N. Candidate genes, genomic instability and cancer progression, Genetics seminar, Tulane University, New Orleans, LA, 03/11

Makridakis N. Error-prone polymerases, genomic instability and prostate cancer progression, COBRE/ External Advisory Board presentation, Tulane University, New Orleans, LA, 03/11

Makridakis N. Single molecule approach detects significant mutation heterogeneity at the androgen receptor locus in prostate tumors, Mutation Detection 2011 meeting, Human Genetics Society of Australasia, Santorini, Greece, 06/11

Makridakis N. Candidate genes, genomic instability and cancer progression, Environmental Health Sciences seminar, Tulane University, New Orleans, LA, 09/11

Makridakis N. Error-prone polymerases, genomic instability and prostate cancer progression, COBRE/ External Advisory Board presentation, Tulane University, New Orleans, LA, 03/12

Makridakis N. Error-prone polymerases, genomic instability and prostate cancer progression, COBRE/ External Advisory Board presentation, Tulane University, New Orleans, LA, 04/13

Funding applied for based on work supported by this award

Makridakis N. Polymerase genes and genomic instability in prostate cancer progression, NCI/R01, 2010

Makridakis N. Identification of common somatic variants of the human POLK gene and its effect on polymerase function, TCC/ Brown Foundation, 2011

Makridakis N. Polymerase beta endonuclease activity and prostate cancer progression, DoD, 2012

Makridakis N. Human DNA polymerases POLB, POLH and POLK and prostate cancer progression, NCI/R01, 2013

CONCLUSION

We identified somatic POLB, POLK, or POLH substitutions in 73% of the prostate cancer patients we examined. Therefore, error-prone polymerase genes are commonly mutated in prostate tumor tissue. However, very few mutations were recurrent. This finding was confirmed by NGS analysis in a different dataset, which uncovered additional, but distinct missense POLB mutations.
Biochemical analysis of the POLB missense variations showed that all of these somatic mutations have functional effects, by either reducing polymerase activity, altering DNA synthesis fidelity (An *et al*, 2011), destabilizing the protein (Figure 1 of Annual report Year 2) or by decreasing a novel endonuclease activity (Figure 6 of Annual report Year 2). The E29K POLK mutation also had functional effects. Thus, this research has uncovered the novel concept that functional alteration of error-prone DNA polymerases may be common and important for prostate cancer progression. Further, we discovered a novel biological activity of Pol β (endonuclease) that is responsible for preventing aneuploidy, an early event in tumor development. In addition, this project led to the characterization of important biomarkers of advanced prostate cancer and early-onset tumors.

"So what?"
Given the prevalence of functional somatic POLB mutations in advanced (invasive) prostate tumors, and the existence of several somatic POLB and POLK mutations in early-onset tumors, we propose that screening for these (and other POLB/POLK) somatic mutations in prostate biopsies may be used as a biomarker for the

detection of presymptomatic or aggressive cancer. However, a DNA sequencing approach may be required (instead of genotyping), since distinct mutations are detected in different datasets. Characterization of the endonuclease activity of the identified POLB mutants, would further benefit patients, as we will understand the clinical effect of these variants in vivo. Eventually, further research can result in the development of mutant specific drugs (such as nucleotide analogs), which would allow better treatment options for these patients.

REFERENCES

An C, Chen D., and Makridakis NM. (2011). Systematic Biochemical Analysis of Somatic Missense Mutations in DNA Polymerase β Found In Prostate Cancer Reveal Alteration of Enzymatic Function. *Hum Mutat,* 32: 415-423.

An C, Beard WA, Chen D, Wilson SA, and Makridakis NM. Understanding the loss of function in a triple missense mutant of DNA polymerase β found in prostate cancer. (*In Press*)

Bebenek K, Garcia-Diaz M, Blanco L, Kunkel TA. (2003). The frameshift infidelity of human DNA polymerase lambda. Implications for function. *J Biol Chem*. 278: 34685-90.

Bergoglio V, Pillaire MJ, Lacroix-Triki M, Raynaud-Messina B, Canitrot Y, Bieth A, Garès M, Wright M, Delsol G, Loeb LA, Cazaux C, Hoffmann JS. (2002). Deregulated DNA polymerase beta induces chromosome instability and tumorigenesis. *Cancer Res*. 62:3511-4.

Fotiadou P, Henegariu O, Sweasy JB. (2004). DNA polymerase beta interacts with TRF2 and induces telomere dysfunction in a murine mammary cell line. *Cancer Res*. 64:3830-7.

Kidane D, Jonason AS, Gorton TS, Mihaylov I, Pan J, Keeney S, de Rooij DG, Ashley T, Keh A, Liu Y, Banerjee U, Zelterman D, Sweasy JB. (2010). DNA polymerase beta is critical for mouse meiotic synapsis. *EMBO J*. 29:410-23.

Luo K, Yuan J, Chen J, Lou Z. (2009). Topoisomerase IIalpha controls the decatenation checkpoint. *Nat Cell Biol*. **11**:204-10.

Makridakis NM, Ferraz L, and Reichardt J KV. (2009). Genomic Analysis of Cancer Tissue Reveals that Somatic Mutations Commonly Occur in a Specific Motif, *Hum Mutat,* 30: 39-48.

Paull TT, Gellert M. (2000). A mechanistic basis for Mre11-directed DNA joining at microhomologies. *Proc Natl Acad Sci U S A*. **97**:6409-14.

APPENDICES:

List:

An C, Beard WA, Chen D, Wilson SA, and Makridakis NM. Understanding the loss of function in a triple missense mutant of DNA polymerase β found in prostate cancer, (*In Press*), 2013

Understanding The Loss Of Function In A Triple Missense Mutant Of DNA Polymerase β Found In Prostate Cancer.

Changlong An[1, 2], William A. Beard[3], Desheng Chen[1]. Samuel H. Wilson[3], and Nick M. Makridakis[1]

[1]Department of Epidemiology and Tulane Cancer Center, Tulane University, New Orleans, LA,

[2]Current address: Department of Physiology & Cell Biology, University of Nevada School of Medicine, Reno, NV

[3]Laborarory of Structural Biology, NIEHS, National Institutes of Health, Research Triangle Park, NC 27709

Address correspondence to: Nick Makridakis, PhD, 1430 Tulane Ave, SL-68, New Orleans, LA 70112, email: nmakrida@tulane.edu

ABSTRACT

Human DNA polymerase (pol) β is essential for base excision repair. We had previously reported a triple missense somatic mutant of pol β (P261L/T292A/I298T) found in an early onset prostate tumor. This mutation abolishes enzyme function, and the wild-type allele was not present in the tumor, indicating a complete deficiency in pol β function. The effect on pol β activity is unexpected because the point mutations that comprise the triple mutant are not part of the active site. Herein we demonstrate the mechanism of this loss of function. In order to understand the effect of the individual point mutations we biochemically analyzed all single and double mutants that comprise the triple mutant. We found that the I298T mutation is responsible for a marked instability of the triple mutant protein at 37 °C. At room temperature the triple mutant's low efficiency is also due to a decrease in the apparent binding affinity for the dNTP substrate, which is due to the T292A mutation. Furthermore, the triple mutant displays lower fidelity for transversions *in vitro*, due to the T292A mutation. We conclude that distinct mutations of the triple pol β mutant are responsible for the loss of activity, lower fidelity, and instability observed *in vitro*.

KEYWORDS: mutagenesis, polymerase, stability, expression analysis, kinetic

1. Introduction

Human DNA polymerase (pol) β is the primary polymerase involved in base excision repair (BER), an essential repair pathway that removes oxidized and alkylated bases from DNA [1]. Its small size and monomeric nature make it an attractive candidate for biochemical and kinetic analysis [2]. DNA polymerase β has also been suggested to be involved in DNA gap-filling reactions during meiotic synapsis [3], the repair of double-strand DNA breaks during non-homologous end joining [4], nucleotide excision repair of bulky DNA lesions [5,6], and replication [7]. Targeted disruption of pol β in mice results in neonatal lethality, growth retardation, and apoptotic cell death in the developing nervous system suggesting a role for pol β in neurogenesis [8].

In contrast to the other human DNA polymerases, the availability of a high-resolution crystal structure of pol β in various liganded states provides a foundation to identify functionally important residues for mechanistic studies, as well as to interpret kinetic results with site-directed mutants. Furthermore, pol β shares many structural and mechanistic features with other DNA polymerases of known structure. For example, the mechanism of DNA polymerization follows an ordered binding of substrates to the enzyme, with the DNA template binding first [9]. These attributes make pol β an excellent model for biochemical study of DNA synthesis and fidelity.

DNA polymerase β lacks a proofreading exonuclease domain, but encompasses two main domains: 1) an amino-terminal 8-kDa lyase domain (responsible for the removal of the 5′-deoxyribose phosphate intermediate formed during BER) and 2) a carboxyl-terminal 31-kDa polymerase domain [10]. The polymerase domain (residues 91-335) can be further separated into three functionally distinct subdomains, which correspond to the palm (catalytic; C), thumb (duplex DNA binding; D) and fingers (dNTP selection or nascent base pair binding; N) subdomains, according to the nomenclature that uses the architectural analogy to a right hand [11].

Comparisons of pol β structures in various liganded states have shown that upon dNTP binding to the binary (pol β/DNA) complex, the N-subdomain rotates from an open to closed state sandwiching the nascent base pair (dNTP-templating nucleotide) between α-helix N and the primer terminus base pair [12,13]. These structures have also shown that productive binding of pol β to both gapped and nicked DNA requires a 90^{o} bend in the DNA template strand at the 5′-phosphodiester linkage of the templating residue. The bend allows residues of the N-subdomain to interact with the nascent base-pair in the closed

conformation (Fig. 1). Various mutagenesis studies have shown that the pol β/dNTP contacts produced by this bend are important for both polymerization efficiency and fidelity (for review, see [2]).

Mutations in the pol β gene are commonly found in tumor tissues [14] and in several instances, these alterations are associated with diminished polymerase fidelity [15], catalytic activity [16], and increase in cellular transformation [17]. By screening the complete coding region of the pol β gene in 26 prostate cancer tissues, we identified 20 somatic mutations, nine of them missense [18]. Subsequent biochemical analysis of all missense pol β mutations demonstrated much smaller changes in enzyme activity for all mutants compared to the triple mutant, P261L/T292A/I298T, which had dramatically decreased activity [19]. The pol β triple mutant was identified in an early-onset prostate cancer patient [18]. No normal allele was present in the patient's tumor, unlike the adjacent normal prostate that was wild type, suggesting a clonal event during tumor evolution. In order to appreciate the significance of the triple mutant, it is essential to understand the molecular mechanism of the effects of the mutations. In addition, information about the structure-activity relationships of the mutations will enhance the understanding of the pol β polymerase activity.

Crystallographic analyses provide insight about the potential importance of the residues altered in the triple mutant. Threonine-292 (Thr292) is a surface exposed residue that is not part of the active site, but hydrogen bonds with the template backbone immediately upstream of the coding templating nucleotide (Fig. 1) [20]. Alanine substitution would abolish this hydrogen bonding interaction, and thus may affect template binding, activity, and/or fidelity. Proline-261 (Pro261) is situated at the boundary between the C- and N-subdomains that reposition themselves in response to nucleotide binding. Isoleucine-298 (Ile298) is distant from the active site and appears to form packing interactions in the mobile N-subdomain (Fig.1). Threonine substitution would result in a buried side chain with hydrogen bonding capacity (Fig.1, right panel). Thus the I298T substitution may alter the folding and/or stability of the N-subdomain. Given these relatively mild consequences expected by the single point mutations that comprise the triple mutant, the complete loss of pol β activity observed previously was unexpected.

We have constructed, purified and biochemically analyzed all single and double mutant variants *in vitro* that comprise the triple mutant in order to understand this apparent paradox regarding the activity of pol β. Herein we demonstrate that the loss of function exhibited by the triple mutant can be separated into distinct enzyme activity and enzyme stability changes, mainly afforded by the T292A and I298T point mutations, respectively.

2. Materials and methods

2.1. Bacterial strains and growth conditions

The strain BL21 DE3 was used for protein expression. *E. coli* DH5α, BL21 (DE3), and recombinant *E. coli* harboring *pol* β genes were cultured in LB medium containing kanamycin (50 μg/ml) when appropriate.

2.2. Construction of pol β variants

Wild-type (WT) *pol* β was obtained from J. Sweasy at Yale University. The mutants were obtained by the Stratagene Quick-change Site-Directed Mutagenesis kit according to the protocol of the manufacturer using the pET28a(+)-WT bacterial expression vector as a template [21]. Successful mutagenesis was confirmed by DNA sequencing with BigDye chemistry on a 3100 ABI sequencer (PerkinElmer).

2.3. Expression and purification of mutant enzymes

E. coli strain BL21 (DE3) carrying pET-28a(+)/Polβ were grown at 37 °C in LB medium containing 50 μg/ml kanamycin with 1 mM IPTG. The cells were harvested by centrifugation, resuspended in 40 mM Tris, pH 8, 500 mM NaCl, 10 mM imidazole, and Protease Inhibitor Cocktail (as recommended by the manufacturer; Sigma). Resuspended cells were lysed by sonication. Extracts were cleared by centrifugation (15,000 rpm, 15 min at 4 °C), and then loaded onto HisTrap FF crude Kit according to the manufacturer instructions (GE Healthcare). Proteins were eluted with 500 mM imidazole in 0.5 M NaCl. The elutants were loaded onto a HiTrap SP HP column (GE Healthcare). The column was washed with 100 mM NaCl and proteins were eluted with 2 M NaCl and stored at -80 °C in 50 mM Tris, pH 8, 1 mM EDTA, 2 M NaCl, 10% glycerol, and protease inhibitors as above [22,23]. We then estimated enzyme homogeneity based on Coomassie Blue-stained SDS-PAGE gels. All proteins were quantified by Bradford protein assay (Sigma).

2.4. Western bloting

Expressed His-tagged proteins were identified by Western blot [24]. Proteins were electrophoresed in a 12% SDS-PAGE gel and transferred to a polyvinylidenedifluoride membrane (Thermo Scientific). Blots were blocked by 5% non-fat dry milk in Tris-buffered saline-Tween 20 (0.1% Tween) and incubated with anti-His Tag antibody (Sigma) according to the protocol of the manufacturer. For detection, we used IRDye 800CW Goat Anti-Rabbit IgG (LI-COR Biosciences) and the Odyssey imaging system (LI-COR Biosciences).

2.5. DNA substrate

All oligonucleotides were synthesized and high-pressure liquid chromatography-purified by Integrated DNA Technologies. A 20-mer primer (5′-GCA GGA AAG CGA GGG TAT CC-3′) and 20-mer downstream oligonucleotide (5′-ACA AAG TCC AGC GTA CCA TA-3′) were annealed to a 46-mer template (5′-TAT GGT ACG CTG GAC TTT GTG GGA TAC CCT CGC TTT CCT GCT CCT G-3′) to generate a one-nucleotide gapped DNA substrate with a templating guanine [25]. The 20-mer primer was 5′-labeled with [γ-^{32}P]ATP (3,000 Ci/mmol; PerkinElmer) using T4 polynucleotide kinase (U. S. Biochemical Corp.) according to the manufacturer's protocol. The 5′-^{32}P labeled primer was then purified from unincorporated label by a Microspin^{TM} G-50 (GE Healthcare) column. The down-stream oligonucleotide was 5′-phosphorylated by Integrated DNA Technologies. The oligonucleotides were annealed at a primer:template:downstream oligonucleotide molar ratio of 1:1.2:1.3 in 50 mM Tris, pH 8.0, 250 mM NaCl, in order to create a single nucleotide gap. The mixture was incubated at 95 °C for 5 min, slow cooled to 50 °C over 30 min, and incubated at 50 °C for 20 min and then transferred to ice. Annealing of primer was confirmed on an 18% polyacrylamide (acrylamide/bis-acrylamide: 29:1) native gel followed by autoradiography as described [26,27].

2.6. Protein stability assay

Protein stability was assessed by incubating pol β for varying lengths of time (3, 6, 9, and 12 min) at 37 °C or room temperature (RT, 22 °C). All reactions (20 µl) were performed in 50 mM Tris-Cl, pH 8.0, 10 mM $MgCl_2$, 2 mM DTT, 20 mM NaCl, 0.2 mg/ml BSA, 2.5% glycerol with 40 nM pol β and 50 nM DNA. All concentrations refer to the final concentration after mixing. The reaction mixtures were pre-incubated in the absence of dCTP and reactions were initiated by the addition of 12.8 µM dCTP. After incubation for 2 min at 37 °C and 6 min at RT, the reactions were quenched by adding 20 µl of formamide loading buffer (900 µl formamide, 22.2 µl 0.5 M EDTA, pH 8.0, and 77.8 µl water) and boiled for 10 min, and then transferred to ice. Products were resolved on a 15% polyacrylamide (acrylamide/bis-acrylamide: 29:1) gel containing 7 M urea. Gels were dried and the products were quantified with a PhosphorImager (Molecular Dynamics).

2.7. Kinetic characterization

The conditions of all incorporation reactions were the same as those described above for the protein stability assay. Kinetic reactions were performed at 37 °C for stable variants and at RT for all variants. To determine $K_{m,dNTP}$, the reaction mixtures contained 2.5 nM purified pol β for correct incorporation and 50 nM pol β for incorrect incorporation with 50 nM annealed DNA substrate. All reactions were performed by first pre-incubating the DNA substrate with pol β for 3 min without dNTPs. Reactions were initiated by the addition of a single dNTP (0.1-2000 µM) and incubated for 2 min at 37 °C (for stable variants) and

for 6 min at RT (for all variants). For $K_{m,DNA}$ determinations, RT reactions contained 20 nM WT or T292A pol β and 40 nM triple mutant; at 37 °C, 8 nM enzyme was used. Reactions were initiated by addition of enzyme mixtures to annealed single-nucleotide gapped DNA substrate (0.01-3.2 μM) and incubated for 4 min at RT or 37 °C. The template nucleotide in the gap was deoxyguanosine and the dCTP concentration was 100 μM. After incubation, the reactions were quenched as described above for the protein stability assay and quantified as above to obtain the percentage of product formed. Time courses were linear for the chosen enzyme concentration and time interval.

2.8. Data analysis

The kinetic data were extracted from Lineweaver–Burk plots. We determined the values of k_{cat} and $K_{m,dNTP}$ from trend line equations calculated from these plots with Microsoft Excel software (Microsoft). Apparent k_{cat} was calculated from V_{max}, where $k_{cat} = V_{max}$/[apparent enzyme]. The apparent enzyme concentration was estimated from total protein. Fidelities for misinsertion reactions were calculated using the following equation: Fidelity = $[(k_{cat}/K_{m,correct}) + (k_{cat}/K_{m,incorrect})]/(k_{cat}/K_{m,incorrect})$.

3. Results

3.1. Triple mutant stability

Variants of a triple mutant of human pol β identified previously in prostate cancer tissues [18] were obtained by site-directed mutagenesis. The WT, triple mutant (P261L/T292A/I298T), and all single and double mutant variants of pol β that comprise the triple mutant were expressed in *E. coli* and purified as described in "Materials and methods." After purification, WT and the variants of pol β were analyzed by SDS-PAGE and identified by Western blot (data not shown), and proteins were quantified by Bradford protein assay. Expression of pol β was poor when the P261L mutation was included in the protein. Thus, P261L, P261L/T292A, P261L/I298T, and triple mutant were partially purified to 49%, 60%, 50%, and 51% homogeneity, respectively. These preparations were devoid of significant contaminating *E. coli* polymerases or exonuclease activities as illustrated by the lack of these activities in the stability measurements described below (Fig. 2). In contrast, the WT, T292A, I298T and T292A/I298T variants were greater than 90% homogenous (data not shown).

Following enzyme purification, we performed assays of pol β activity by using a DNA substrate that was previously used for pol β fidelity studies [25]. We determined pol β catalytic efficiency based on kinetic analyses of single-nucleotide addition opposite template dG with single-nucleotide gapped DNA substrate. Since the catalytic efficiency ($k_{cat}/K_{m,dCTP}$) of the triple mutant on a gapped DNA substrate was dramatically reduced at 37 °C (Fig. 2) and it was difficult to purify the triple mutant to more than 50%

homogeneity, we hypothesized that this mutant may be unstable at 37 °C and was degraded during bacterial expression.

To probe this hypothesis, we tested the stability of WT and all single, double and triple mutant variants of pol β by examining the sensitivity of the dCTP incorporation reaction to incubation time at 37 °C. Interestingly, the triple mutant, I298T, P261L/I298T, and T292A/I298T variants are unstable at 37 °C: after 3 min of pre-incubation at 37 °C, the activity of those variants was dramatically decreased (Fig. 2*A*–*C*). In contrast, the P261L/T292A variant and its respective single mutant variants are stable at 37 °C (Fig. 2*C* and data not shown). These results suggest that the stability of the triple mutant at 37 °C was affected specifically by the I298T alteration. At room temperature, the stability of the triple mutant is increased and comparable to WT (Fig. 2*D*). Since several of the mutant forms (e.g., I298T, P261L/I298T, T292A/I298T, P261L/T292A/I298T) do not exhibit activity at long incubation periods at 37 °C, these preparations provide an opportunity to ascertain whether contaminating activities exist. The lack of *any* activity indicates that *E. coli* polymerases do not contribute to product formation in these preparations at room temperature and that our purification protocol removes contaminating polymerase activities from our enzyme preparations.

3.2. Catalytic efficiencies for correct incorporation

Following the confirmation of decreased stability conferred by the triple mutant, we decided to test whether stability alone explains the dramatic reduction in activity at 37 °C (Fig. 2), by measuring the steady-state kinetic parameters for all of the variants at room temperature (Table 1; Fig. 3, left panel). As expected, the apparent k_{cat} values of the pol β variants that could be measured at 37 °C (Table 2) were lower at room temperature.

Since both the triple mutant and all I298T containing variants are unstable at 37 °C, we assayed these variants at room temperature to ascertain if the modified side chains had kinetic consequences other than reducing protein stability. Variants of triple mutant, I298T, and P261L/I298T displayed a moderately reduced apparent k_{cat} at RT compared with WT, whereas the T292A/I298T variant showed similar catalytic activity to that of WT pol β at RT (Table 1). Since the active fraction of enzyme is unknown in these preparations, it is difficult to come to any definitive conclusions concerning activity alone. However, both the apparent K_m and the catalytic efficiency (k_{cat}/K_m) values are independent of active enzyme fraction and thus constitute convenient kinetic parameters to monitor altered kinetic constants [28]. The apparent $K_{m,dCTP}$ of the triple mutant, T292A/I298T, and P261L/I298T variants were increased at room

temperature 40-fold, 10-fold, and 3-fold, respectively, compared to WT (Table 1). At 37 °C, the apparent $K_{m,dCTP}$ of the triple mutant was increased 15-fold compared to WT, similar to the change observed at RT (Table 2). Likewise, the $K_{m,dCTP}$ of the T292A and P261L/T292A variants were significantly increased at both RT and 37 °C relative to WT (Table 1 and Table 2).

A comparison of the catalytic efficiencies or specificity constants for WT and the variants at RT indicates that the triple mutant exhibits the lowest catalytic efficiency for correct nucleotide insertion and P261L has similar or greater efficiency than WT (Table 1; Fig. 3, left panel). The catalytic efficiencies for the other variants were intermediate between these two extremes (Table 1; Fig. 3, left panel). Significantly, all T292A-containing variants reduced catalytic efficiency compared to WT at RT: the T292A variant (by 3.3-fold), the P261L/T292A variant (by 9.4-fold) and the T292A/I298T variant (by 10.4-fold) (Table 1). In addition, the P261L/I298T variant decreased catalytic efficiency at RT by 3.9-fold (Table 1). These differences are most easily seen in Figure 3 where the catalytic efficiencies for correct insertion (dCTP, black lines) are plotted for WT and each variant (note the logarithmic ordinate scale). Therefore, the triple mutant affects catalysis independently of its effect on stability. Due to the lack of protein stability, we did not measure kinetic parameters for any of the I298T containing mutants at 37 °C. The triple mutant displays a catalytic efficiency for correct insertion 3000-fold lower than WT at 37 °C [19] (Table 2; Fig. 3, right panel). The catalytic efficiency of the remaining mutants, P261L, T292A, and P261L/T292A was similar to that of WT at 37 °C (Table 2 and Fig. 3, right panel).

3.3. Fidelity of the pol β variants

Misincorporation fidelity studies were performed to understand the role of the pol β variants on DNA synthesis fidelity. The apparent k_{cat}, $K_{m,dNTP}$, and catalytic efficiency ($k_{cat}/K_{m,dNTP}$) values for misincorporation at room temperature and 37 °C are tabulated in Tables 1 and 2, respectively. The instability of the I298T variants at 37 °C precluded fidelity assays for many of the variants at the elevated temperature. The catalytic efficiencies for misinsertion are also illustrated in discrimination plots (Fig. 3) and their relative fidelities (mutant/WT) shown in Figure 4. In discrimination plots, the distance between correct insertion (black lines) to that of a misinsertion (colored lines) is directly proportional to fidelity or misinsertion frequency [29]. Accordingly, the shorter the distance between these points (correct insertion and misinsertion), the lower the fidelity. For example, focusing on the kinetic constants shown in Figure 3 for the P261L mutant indicates that fidelity for all three misinsertions is greater than that for WT (*e.g.,* efficiency for dCTP insertion is increased relative to WT and misinsertions are reduced compared to WT).

We were unable to measure the catalytic activity for dTTP and dGTP misincorporation for the triple mutant due to its very low misinsertion efficiency (even at very high enzyme concentrations). With regards to catalytic efficiency for misincorporation ($k_{cat}/K_{m,dNTP}$), the $k_{cat}/K_{m,dNTP}$ for the T292A variant was increased for both dATP and dGTP misincorporations and decreased for dTTP. The remaining variants showed decreased catalytic efficiencies for all misincorporations (Table 1, Fig. 3). The results of misincorporation at 37 °C are tabulated in Table 2 and illustrated in Figure 3 (right panel). For the variants that could be examined, the results parallel those observed at room temperature (Fig. 3, left panel).

Fidelity is defined as the ratio of the sum of catalytic efficiencies of correct and incorrect nucleotide incorporation over the catalytic efficiency for misinsertion. Since the efficiency for misinsertion is much lower than that for correct insertion (Tables 1 and 2), a simplified view is that fidelity is simply the ratio of catalytic efficiencies (correct/incorrect). As explained above, the distance between the plotted catalytic efficiencies for correct and incorrect insertions is directly proportional to fidelity (Fig. 3). The relative fidelities (mutant/WT) can easily be illustrated (Fig. 4). The triple mutant has a 7-fold lower fidelity than WT for dATP transversions at room temperature. In contrast, the P261L variant had a significantly higher fidelity than WT at both room temperature and 37 °C. The I298T and P261L/I298T variants also exhibited a higher fidelity at room temperature for all three misinsertions that were assayed.

The T292A variant had decreased relative misinsertion fidelity for dATP and dGTP at room temperature and 37 °C (Fig. 4), and an increased relative fidelity for dTTP at both temperatures Thus, the T292A variant displays higher relative fidelity for transitions and lower relative fidelity for transversions. The P261L/T292A and T292A/I298T variants (both containing T292A) behave like the T292A variant (Fig. 4). Indeed, although the P261L and I298T variants have higher relative fidelity for dATP and dGTP misincorporation compared to the T292A variant, the T292A appears to be dominant over the other mutation in the double mutants P261L/T292A and T292A/I298T.

3.4. Apparent DNA substrate binding

Given the dramatic effect of the triple and T292A mutations on the apparent $K_{m,dCTP}$ (Tables 1 and 2) and the structural observation that Thr292 forms a hydrogen bond with template strand (Fig. 1), we investigated its effect on the affinity for the gapped DNA substrate. A steady-state kinetic analysis indicates that DNA binding is weaker for these mutants (Table 3) and that the elevated $K_{m,dCTP}$ is in part due to weaker DNA binding [28]. Accordingly, the poor catalytic efficiency of the triple mutant at room temperature is in part due to its poor DNA binding.

4. Discussion

Biochemical analyses of all the single and double mutant variants that comprise the triple pol β mutant demonstrate that the complete loss of function shown by the triple mutant can be separated into distinct enzyme activity and stability changes. More specifically, the I298T pol β variant is responsible for the instability shown by the triple mutant at 37 °C (Fig. 2), while the T292A variant is responsible for the loss of DNA synthesis fidelity (Fig. 4), and most of the reduction in catalytic efficiency seen at RT (Fig.3, left panel). The third variant, P261L, exhibits a modest increase in fidelity relative to WT enzyme. Interestingly, all three alterations of the triple mutant are in the same pol β subdomain (N-subdomain; Fig. 1). The N-subdomain (residues 261-335) undergoes a large conformational change upon dNTP binding to interact with the nascent base pair [2]. Accordingly, alterations to this subdomain that interfere with conformational changes/adjustments or interactions with the nascent base pair would be expected to impact enzyme activity and/or fidelity.

The dramatic effect of the I298T pol β variant on enzyme stability observed at 37 °C was surprising, but can be rationalized in considering the pol β structure (Fig. 1). The hydrophobic isoleucine residue found in the wild-type enzyme would be expected to provide good packing for the interior of the N-subdomain. The threonine substitution buries a hydroxyl group that would be expected to lower the stability of this subdomain. Also noteworthy, residues 292 and 298 are adjacent to one another in anti-parallel β-strands (Fig. 1). Thus, the loss of activity at 37 °C is most easily explained by the decreased stability of the N-subdomain with the I298T substitution. Since there is activity, albeit low, at room temperature, the N-subdomain must be at least partially folded at the lower temperature to permit interactions with the nascent base pair. Previous work had demonstrated that loss of the Arg283 interaction with the template strand by site-directed mutagenesis results in a >30,000-fold loss in catalytic efficiency [30,31]. In light of such a dramatic effect, the decrease in catalytic efficiency afforded by the triple mutant is in reasonable context.

Although the I298T variants are unstable at 37 °C, they exhibit significant activity at room temperature permitting kinetic characterization (Table 1). While the activity of the pol β variants assayed at RT was similar to wild-type enzyme, catalytic efficiency was significantly decreased for the triple mutant and all T292A-containing variants (Table 1; Fig.3, left panel), mostly due to a significant increase in the apparent $K_{m,dNTP}$ (Table 1). The $K_{m,dNTP}$ can increase due to an increase in the dissociation constant $K_{d,dNTP}$, decreased rate of dNTP insertion, or decreased DNA binding affinity (*i.e.,* increased dissociation rate

constant, k_{off}) [28]. The T292A substitution is predicted to eliminate an important hydrogen bond with the DNA backbone immediately upstream of the templating (coding) nucleotide (Fig. 1). The observed increase in $K_{m,dNTP}$ for the T292A variants may thus be partially due to decreased DNA binding affinity and is consistent with the observed increased catalytic activity of these variants (Table 1) since increasing the DNA dissociation rate constant can enhance catalytic cycling [32]. Consistent with this idea, the $K_{m,DNA}$ for the T292A variant and triple mutant are increased relative to wild-type enzyme (Table 3). The triple mutant was previously identified as a somatic mutation in a prostate tumor and exhibited reduced enzyme activity. The poor DNA binding of the triple mutant would be expected to result in a base excision repair defect resulting in genomic accumulation of simple base lesions. Alternatively, a less faithful DNA polymerase may fulfill gap-filling DNA synthesis during repair. Previously it was shown that the loss of pol β function in mouse embryonic fibroblasts results in an increase in spontaneous and alkylation-induced mutation frequency [33].

Since DNA synthesis fidelity approximates the ratio of catalytic efficiencies for right and wrong nucleotides, these efficiencies must be differentially altered for a variant polymerase to exhibit an altered fidelity. There are several examples where mutations distant from the pol β active site have impacted DNA synthesis fidelity [2]. The only single nucleotide alteration of the triple mutant that directly contacts the DNA substrate, T292A, exhibits a significantly lower fidelity for transversions (dATP and dGTP misinsertions opposite dG; Figs. 3 and 4). Importantly, the double mutants containing T292A (P261L/T292A and T292A/I298T) also exhibit the transversion over transition bias. The triple mutant likewise exhibits a lower fidelity than WT for dATP misinsertion opposite G. Interestingly, the P261L single mutant has a significantly higher fidelity than WT at room temperature and 37 °C, but the P261L/T292A double mutant does not. These data suggest that the T292A mutation is dominant compared to both P261L and I298T with regards to fidelity. Several previously characterized pol β mutants, including some found in tumors, exhibit a base substitution bias. For example, the D246V pol β mutant, present in the flexible loop in the catalytic C-subdomain (Fig. 1), shows a preferential misinsertion of dTTP opposite guanine relative to WT [34]. This misincorporation bias makes the D246V enzyme a mutator mainly for C to T transitions. In contrast, all of the remaining pol β mutants we identified in prostate tumors do not exhibit this bias [19]. However, fidelity is dependent on DNA sequence and dNTP pool imbalances, so a strict correlation between *in vitro* polymerase fidelity measurements with altered polymerases and their cellular impact on mutagenesis is qualitative.

Crystallographic analyses of pol β have shown that productive binding of pol β to both gapped and nicked DNA template requires a 90^o bend in the DNA template [12,13]. This 90^o bend allows α-helix N residues

of the N-subdomain of pol β to interact with the nascent base-pair in the closed conformation (Fig. 1). Various mutagenesis studies have shown that the pol β/dNTP contacts produced by this 90^{o} bend are important for both polymerization efficiency and fidelity [10,30,32]. Thus, residues that influence the equilibrium between the open and closed forms could potentially modulate enzyme activity or fidelity if they were modified. Thr292 is far from the template strand in the open binary DNA complex, but as discussed above, the hydrogen bond between Thr292 and the template strand would be expected to stabilize the closed pol β form as well as assist template base positioning. Consistent with this prediction, removal of this hydrogen bond through alanine substitution (T292A) results in increases of both the apparent K_m for the DNA and the incoming dNTP. Curiously, Pro261 is situated at the boundary between the C- and N-subdomains, at a position critical for the transition from open to closed form [2,13]. The observation that leucine substitution of Pro261 increases fidelity of the mutant due to a decrease in catalytic efficiency for misinsertions (Fig. 3) suggests that the closed conformation is destabilized in the P261L mutant during incorrect nucleotide incorporation.

In summary, the *in vitro* kinetic analyses presented here demonstrate that the complete loss of function shown by the pol β early onset prostate tumor-associated triple mutant can be separated into distinct changes in catalytic efficiency and fidelity (primarily the T292A point mutation) as well as an enzyme stability defect (I298T mutation). The results explain the mechanistic underpinning of the dramatic loss in enzymatic activity of this tumor-associated mutant form of pol β. The fact that the wild-type allele of pol β was not found in the tumor indicates that this tumor was pol β null. The pro-mutagenesis and therapeutic implications of this are interesting to consider.

Acknowledgments

This research was supported by Research Project Numbers Z01-ES050158 and Z01-ES050161 in the Intramural Research Program of the National Institutes of Health, National Institute of Environmental Health Sciences and was in association with the National Institutes of Health Grant 1U19CA105010. NMM is supported by grant number P20RR020152-06 from the National Institutes of Health, and PC094628 from the Department of Defense. Molecular graphics images were produced using the Chimera package [35] from the Resource for Biocomputing, Visualization, and Informatics at the University of California, San Francisco (supported by NIH P41 RR-01081).

Conflict of interest statement

The authors declare that there are no conflicts of interest.

References

[1] E.C. Friedberg DNA damage and repair, Nature 421 (2003) 436-440.

[2] W.A. Beard, S.H. Wilson Structure and mechanism of DNA polymerase β, Chem. Rev. 106 (2006) 361-382.

[3] D. Kidane, A.S. Jonason, T.S. Gorton, I. Mihaylov, J. Pan, S. Keeney, D.G. de Rooij, T. Ashley, A. Keh, Y. Liu, U. Banerjee, D. Zelterman, J.B. Sweasy DNA polymerase β is critical for mouse meiotic synapsis, EMBO J 29 (2010) 410-423.

[4] T.E. Wilson, M.R. Lieber Efficient processing of DNA ends during yeast nonhomologous end joining: Evidence for a DNA polymerase β (POL4)-dependent pathway, J. Biol. Chem. 274 (1999) 23599-23609.

[5] J.K. Horton, D.K. Srivastava, B.Z. Zmudzka, S.H. Wilson Strategic down-regulation of DNA polymerase β by antisense RNA sensitizes mammalian cells to specific DNA damaging agents, Nucleic Acids Res. 23 (1995) 3810-3815.

[6] N. Oda, J.K. Saxena, T.M. Jenkins, R. Prasad, S.H. Wilson, E.J. Ackerman DNA polymerases α and β are required for DNA repair in an efficient nuclear extract from Xenopus oocytes, J. Biol. Chem. 271 (1996) 13816-13820.

[7] T.M. Jenkins, J.K. Saxena, A. Kumar, S.H. Wilson, E.J. Ackerman DNA polymerase β and DNA synthesis in Xenopus oocytes and in a nuclear extract, Science 258 (1992) 475-478.

[8] N. Sugo, Y. Aratani, Y. Nagashima, Y. Kubota, H. Koyama Neonatal lethality with abnormal neurogenesis in mice deficient in DNA polymerase β, EMBO J. 19 (2000) 1397-1404.

[9] K. Tanabe, E.W. Bohn, S.H. Wilson Steady-state kinetics of mouse DNA polymerase β, Biochemistry 18 (1979) 3401-3406.

[10] W.A. Beard, D.D. Shock, X.-P. Yang, S.F. DeLauder, S.H. Wilson Loss of DNA polymerase β stacking interactions with templating purines, but not pyrimidines, alters catalytic efficiency and fidelity, J. Biol. Chem. 277 (2002) 8235-8242.

[11] D.L. Ollis, P. Brick, R. Hamlin, N.G. Xuong, T.A. Steitz Structure of large fragment of Escherichia coli DNA polymerase I complexed with dTMP, Nature 313 (1985) 762-766.

[12] H. Pelletier, M.R. Sawaya, W. Wolfle, S.H. Wilson, J. Kraut Crystal structures of human DNA polymerase β complexed with DNA: Implications for catalytic mechanism, processivity, and fidelity, Biochemistry 35 (1996) 12742-12761.

[13] M.R. Sawaya, P. Prasad, S.H. Wilson, J. Kraut, H. Pelletier Crystal structures of human DNA polymerase β complexed with gapped and nicked DNA: Evidence for an induced fit mechanism, Biochemistry 36 (1997) 11205-11215.

[14] D. Starcevic, S. Dalal, J.B. Sweasy Is there a link between DNA polymerase β and cancer?, Cell Cycle 3 (2004) 998-1001.

[15] T. Lang, M. Maitra, D. Starcevic, S.-X. Li, J.B. Sweasy A DNA polymerase β mutant from colon cancer cells induces mutations, Proc. Natl. Acad. Sci. USA 101 (2004) 6074-6079.

[16] T. Lang, S. Dalal, A. Chikova, D. DiMaio, J.B. Sweasy The E295K DNA polymerase Beta gastric cancer-associated variant interferes with base excision repair and induces cellular transformation, Mol. Cell. Biol. 27 (2007) 5587-5596.

[17] J.B. Sweasy, T. Lang, D. Starcevic, K.-W. Sun, C.-C. Lai, D. DiMaio, S. Dalal Expression of DNA polymerase β cancer-associated variants in mouse cells results in cellular transformation, Proc. Natl. Acad. Sci. USA 102 (2005) 14350-14355.

[18] N.M. Makridakis, L.F.C. Ferraz, J.K.V. Reichardt Genomic analysis of cancer tissue reveals that somatic mutations commonly occur in a specific motif, Hum. Mutat. 30 (2009) 39-48.

[19] C.L. An, D. Chen, N.M. Makridakis Systematic biochemical analysis of somatic missense mutations in DNA polymerase β found in prostate cancer reveal alteration of enzymatic function, Hum. Mutat. 32 (2011) 415-423.

[20] V.K. Batra, W.A. Beard, D.D. Shock, J.M. Krahn, L.C. Pedersen, S.H. Wilson Magnesium induced assembly of a complete DNA polymerase catalytic complex, Structure (Camb) 14 (2006) 757-766.

[21] S. Dalal, S. Hile, K.A. Eckert, K.-w. Sun, D. Starcevic, J.B. Sweasy Prostate-cancer-associated I260M variant of DNA polymerase β is a sequence-specific mutator, Biochemistry 44 (2005) 15664-15673.

[22] C.L. An, W.J. Lim, S.Y. Hong, E.J. Kim, E.C. Shin, M.K. Kim, J.R. Lee, S.R. Park, J.G. Woo, Y.P. Lim, H.D. Yun Analysis of bgl operon structure and characterization of β-glucosidase from Pectobacterium carotovorum subsp. carotovorum LY34, Biosci. Biotechnol. Biochem. 68 (2004) 2270-2278.

[23] J.L. Kosa, J.B. Sweasy 3'-Azido-3'-deoxythymidine-resistant mutants of DNA polymerase β identified by in vivo selection, J. Biol. Chem. 274 (1999) 3851-3858.

[24] L. Servant, C. Cazaux, A. Bieth, S. Iwai, F. Hanaoka, J.-S. Hoffmann A role for DNA polymerase β in mutagenic UV lesion bypass, J. Biol. Chem. 277 (2002) 50046-50053.

[25] A.M. Chagovetz, J.B. Sweasy, B.D. Preston Increased activity and fidelity of DNA polymerase β on single-nucleotide gapped DNA, J. Biol. Chem. 272 (1997) 27501-27504.

[26] S.X. Li, J.A. Vaccaro, J.B. Sweasy Involvement of phenylalanine 272 of DNA polymerase beta in discriminating between correct and incorrect deoxynucleoside triphosphates, Biochemistry 38 (1999) 4800-4808.

[27] M. Maitra, A. Gudzelak, Jr., S.-X. Li, Y. Matsumoto, K.A. Eckert, J. Jager, J.B. Sweasy Threonine 79 is a hinge residue that governs the fidelity of DNA polymerase β by helping to position the DNA within the active site, J. Biol. Chem. 277 (2002) 35550-35560.

[28] W.A. Beard, K. Bebenek, T.A. Darden, L. Li, R. Prasad, T.A. Kunkel, S.H. Wilson Vertical-scanning mutagenesis of a critical tryptophan in the minor groove binding track of HIV-1 reverse

transcriptase: Molecular nature of polymerase-nucleic acid interactions, J. Biol. Chem. 273 (1998) 30435-30442.

[29] W.A. Beard, V.K. Batra, S.H. Wilson DNA polymerase structure-based insight on the mutagenic properties of 8-oxoguanine, Mutat. Res. 703 (2010) 18-23.

[30] W.A. Beard, W.P. Osheroff, R. Prasad, M.R. Sawaya, M. Jaju, T.G. Wood, J. Kraut, T.A. Kunkel, S.H. Wilson Enzyme-DNA interactions required for efficient nucleotide incorporation and discrimination in human DNA polymerase β, J. Biol. Chem. 271 (1996) 12141-12144.

[31] W.A. Beard, D.D. Shock, B.J. Vande Berg, S.H. Wilson Efficiency of correct nucleotide insertion governs DNA polymerase fidelity, J. Biol. Chem. 277 (2002) 47393-47398.

[32] B.J. Vande Berg, W.A. Beard, S.H. Wilson DNA structure and aspartate 276 influence nucleotide binding to human DNA polymerase β: Implication for the identity of the rate-limiting conformational change, J. Biol. Chem. 276 (2001) 3408-3416.

[33] R.W. Sobol, D.E. Watson, J. Nakamura, F.M. Yakes, E. Hou, J.K. Horton, J. Ladapo, B. Van Houten, J.A. Swenberg, K.R. Tindall, L.D. Samson, S.H. Wilson Mutations associated with base excision repair deficiency and methylation-induced genotoxic stress, Proc. Natl. Acad. Sci. USA 99 (2002) 6860-6865.

[34] S. Dalal, J.L. Kosa, J.B. Sweasy The D246V mutant of DNA polymerase β misincorporates nucleotides: Evidence for a role for the flexible loop in DNA positiining within the active site, J. Biol. Chem. 279 (2004) 577-584.

[35] E.F. Pettersen, T.D. Goddard, C.C. Huang, G.S. Couch, D.M. Greenblatt, E.C. Meng, T.E. Ferrin UCSF Chimera—A visualization system for exploratory research and analysis, J. Comput. Chem. 25 (2004) 1605-1612.

[36] R.L. Dunbrack, Jr. Rotamer libraries in the 21st century, Curr. Opin. Struct. Biol. 12 (2002) 431-440.

FIGURE LEGENDS

FIGURE 1. Position of the variant residues of the triple mutant in the structure of the DNA polymerase β ternary substrate complex. *Left panel*, a ribbon representation of pol β illustrating the polymerase (colored) and amino-terminal lyase (grey) domains (PDB code 2FMS). The polymerase domain is composed of three subdomains: D, purple; C, gold; and N, green. These correspond to the thumb, palm, and fingers subdomains of DNA polymerases that utilize an architectural analogy to a right-hand, respectively. The single-nucleotide gapped DNA is illustrated in a ladder representation with a red template strand and blue primer and downstream DNA strands. The 5′-end of the template strand is indicated. The nascent base pair (templating nucleotide and incoming nucleoside triphosphate) is shown in a stick representation with a mesh surface. The three residues (Pro261, P261; Thr292, T292; and Ile298, I298) of the N-subdomain altered in the triple mutant and α-helix N are shown. *Right panel*, the molecular surface of the N-subdomain is clipped to expose the internal position of the altered Thr298 (T298) and the surface exposed Ala292 (A292). The altered residues are shown in magenta as ball-and-sticks and their contribution to the surface is also shaded in magenta. Although the residue cannot be seen in this view, the surface contribution of Leu261 (L261) is indicated. The altered side chains were modeled based on probable rotamers from the Dunbrack library [36] and exhibited no clashes with nearby residues. The red template strand in the vicinity of the N-subdomain is also shown and α-helix N that interacts with the nascent base pair is labeled. The molecular images were produced in Chimera [35].

FIGURE 2. Stability of the DNA polymerase β variants. The stability of the pol β variants was assessed by activity after incubation at 37 °C (panels *A*–*C*) or room temperature (22 °C, panel *D*) for various lengths of time as described under "Materials and Methods." The panels show autoradiographes of gels depicting substrate (faster migrating band) and products (slower migrating band). The position of the ^{32}P-labeled substrate band without extension (–E) is shown at the left. The stability of the triple mutant is compared to that of wild-type (WT) enzyme in panels *A* and *D*. The stability of I298T and the double mutants (P261L/T292A, P261L/I298T, and T292A/I298T) are compared to WT in panels *B* and *C*, respectively. The pre-incubation time intervals (min) are indicated above the respective lanes and refer to the period that enzyme and DNA were incubated before initiating the reaction with dCTP.

FIGURE 3. Discrimination plot for DNA polymerase β and its variants. The catalytic efficiencies for correct insertion (dCTP, black lines) and incorrect insertion (dATP, red lines; dGTP, green lines; and dTTP, purple lines) opposite a templating guanine are plotted for each enzyme. The catalytic efficiencies for room temperature (22 °C, *left panel*) and 37 °C (*right panel*) are taken from Tables 1 and 2, respectively. Discrimination or fidelity is determined from the ratio of catalytic efficiencies for competing substrates (e.g., right versus wrong nucleotide insertion). Accordingly, plots of the log of these catalytic efficiencies illustrate the difference (i.e., magnitude of discrimination/fidelity is directly proportional to the distance between the black line and the respective colored lines). The asterisks indicate that the catalytic efficiencies could not be determined due to the low stability of these variants.

FIGURE 4. Relative fidelity of the DNA polymerase β variants. Relative fidelities (dATP, open bars; dGTP, dark grey bars; dTTP, light grey bars) opposite a templating guanine were calculated from the ratio of fidelities (variant/wild type) determined at room temperature (22 °C, *left panel*) and 37 °C (*right panel*). The asterisks indicate that the catalytic efficiencies could not be determined due to the low stability of these variants.

TABLE 1

Kinetic summary for single-nucleotide gap-filling opposite a templating guanine at room temperature (22 °C) by wild-type pol β and variants.

The results represent the mean (SD) of at least three independent determinations.

Enzyme	dNTP	k_{cat}[a]		$K_{m,dNTP}$		k_{cat}/K_m	
		10^{-2} s^{-1}		μM		10^{-2} $\mu M^{-1}s^{-1}$	
WT[b]	dCTP	3.24	(0.27)	0.42	(0.04)	771	(150)
P261L		5.57	(0.33)	0.39	(0.04)	1430	(80)
T292A		4.98	(0.13)	2.16	(0.16)	231	(11)
I298T		1.35	(0.30)	0.24	(0.03)	563	(51)
P261L/T292A		4.98	(0.52)	6.06	(0.20)	82	(8)
P261L/I298T		2.50	(0.27)	1.25	(0.10)	200	(27)
T292A/I298T		3.25	(0.08)	4.38	(0.35)	74	(9)
TM[c]		2.36	(0.34)	17.08	(4.48)	14	(1)
WT	dATP	0.164	(0.012)	131	(22)	0.125	(0.029)
P261L		0.135	(0.005)	331	(14)	0.041	(0.001)
T292A		0.223	(0.010)	98	(11)	0.227	(0.015)
I298T		0.091	(0.006)	397	(64)	0.023	(0.003)
P261L/T292A		0.095	(0.001)	195	(21)	0.049	(0.008)
P261L/I298T		0.037	(0.005)	244	(44)	0.015	(<0.001)
T292A/I298T		0.125	(0.018)	373	(60)	0.035	(0.002)
TM		0.046	(0.002)	282	(27)	0.016	(0.002)
WT	dGTP	0.110	(0.007)	787	(55)	0.014	(0.001)
P261L		0.211	(0.069)	3036	(1397)	0.007	(0.001)
T292A		0.113	(0.009)	531	(44)	0.021	(<0.001)
I298T		0.064	(0.006)	880	(262)	0.007	(0.001)
P261L/T292A		0.024	(0.003)	293	(66)	0.008	(0.001)
P261L/I298T		0.055	(0.010)	2205	(589)	0.003	(<0.001)
T292A/I298T		0.019	(0.002)	293	(80)	0.006	(0.002)
TM		ND[d]		ND		ND	
WT	dTTP	0.244	(0.008)	275	(52)	0.089	(0.013)
P261L		0.143	(0.017)	665	(65)	0.021	(0.001)
T292A		0.110	(0.021)	822	(164)	0.013	(0.001)
I298T		0.089	(0.026)	424	(188)	0.021	(0.003)
P261L/T292A		0.017	(0.001)	367	(75)	0.005	(0.001)
P261L/I298T		0.019	(0.002)	1068	(77)	0.002	(<0.001)
T292A/I298T		0.017	(0.003)	483	(102)	0.004	(0.001)
TM		ND		ND		ND	

[a]Apparent k_{cat} was calculated from V_{max}, where $k_{cat} = V_{max}$/[apparent enzyme]. The apparent enzyme concentration was estimated from total protein.

[b]Wild-type human DNA polymerase β.

[c]Triple mutant (P261L/T292A/I298T) of human DNA polymerase β.

[d]Not determined.

TABLE 2

Kinetic summary for single-nucleotide gap-filling opposite a templating guanine at 37 ˚C by wild-type pol β and variants.

The results represent the mean (SD) of at least three independent determinations.

Enzyme	dNTP	k_{cat}[a]	$K_{m,dNTP}$	k_{cat}/K_m
		10^{-2} s^{-1}	μM	10^{-2} $\mu M^{-1}s^{-1}$
WT[b]	dCTP	8.09 (2.09)	0.25 (0.10)	3240 (920)
P261L		13.6 (0.9)	0.29 (0.07)	4690 (1450)
T292A		17.3 (1.2)	0.68 (0.28)	2540 (730)
I298T		ND[c]	ND	ND
P261L/T292A		25.6 (1.2)	1.08 (0.15)	2370 (300)
P261L/I298T		ND	ND	ND
T292A/I298T		ND	ND	ND
TM[d]		0.040 (0.003)	3.72 (0.17)	1.08 (0.08)
WT	dATP	0.786 (0.012)	47 (2)	1.680 (0.093)
P261L		0.630 (0.024)	114 (5)	0.553 (0.026)
T292A		0.846 (0.048)	33 (2)	2.557 (0.032)
I298T		ND	ND	ND
P261L/T292A		0.792 (0.037)	59 (4)	1.348 (0.019)
P261L/I298T		ND	ND	ND
T292A/I298T		ND	ND	ND
TM		ND	ND	ND
WT	dGTP	0.587 (0.001)	446 (16)	0.131 (0.005)
P261L		0.527 (0.062)	1069 (223)	0.049 (0.005)
T292A		0.709 (0.032)	376 (42)	0.189 (0.015)
I298T		ND	ND	ND
P261L/T292A		0.490 (0.017)	586 (25)	0.084 (0.001)
P261L/I298T		ND	ND	ND
T292A/I298T		ND	ND	ND
TM		ND	ND	ND
WT	dTTP	0.870 (0.012)	52 (2)	1.667 (0.030)
P261L		0.702 (0.028)	152 (15)	0.460 (0.030)
T292A		0.715 (0.048)	491 (43)	0.146 (0.005)
I298T		ND	ND	ND
P261L/T292A		0.410 (0.011)	569 (34)	0.072 (0.003)
P261L/I298T		ND	ND	ND
T292A/I298T		ND	ND	ND
TM		ND	ND	ND

[a]Apparent k_{cat} was calculated from V_{max}, where $k_{cat} = V_{max}$/[apparent enzyme]. The apparent enzyme concentration was estimated from total protein.

[b]Wild-type human DNA polymerase β.

[c]Not determined due to the poor stability of the protein.

[d]Triple mutant (P261L/T292A/I298T) of human DNA polymerase β.

TABLE 3

Dependence of DNA synthesis on single-nucleotide gapped DNA concentration at room temperature and 37 ˚C by wild-type pol β and variants.

The results represent the mean (SD) of at least three independent determinations. The templating base in the gap was guanine and the dCTP concentration was 100 μM.

Enzyme	Temperature	k_{cat}[a]	$K_{m,DNA}$	k_{cat}/K_m
		10^{-2} s^{-1}	μM	10^{-2} $\mu M^{-1}s^{-1}$
WT[b]	RT	7.8 (0.2)	0.16 (0.01)	4875 (75)
	37 °C	9.8 (0.5)	0.07 (<0.01)	14000 (240)
TM[c]	RT	40.4 (2.0)	1.5 (0.1)	2700 (20)
	37 °C	ND[d]	ND	ND
T292A	RT	3.6 (0.1)	0.25 (0.02)	1440 (40)
	37 °C	38.6 (7.3)	1.48 (0.32)	2610 (60)

[a]Apparent k_{cat} was calculated from V_{max}, where $k_{cat} = V_{max}$/[apparent enzyme]. The apparent enzyme concentration was estimated from total protein.

[b]Wild-type human DNA polymerase β.

[c]Triple mutant (P261L/T292A/I298T) of human DNA polymerase β.

[d]Not determined.

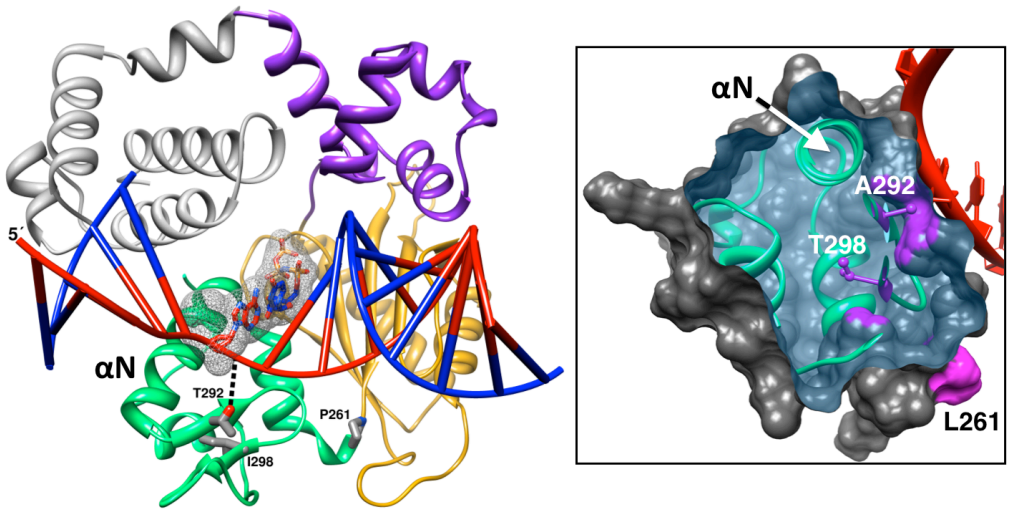

FIGURE 1

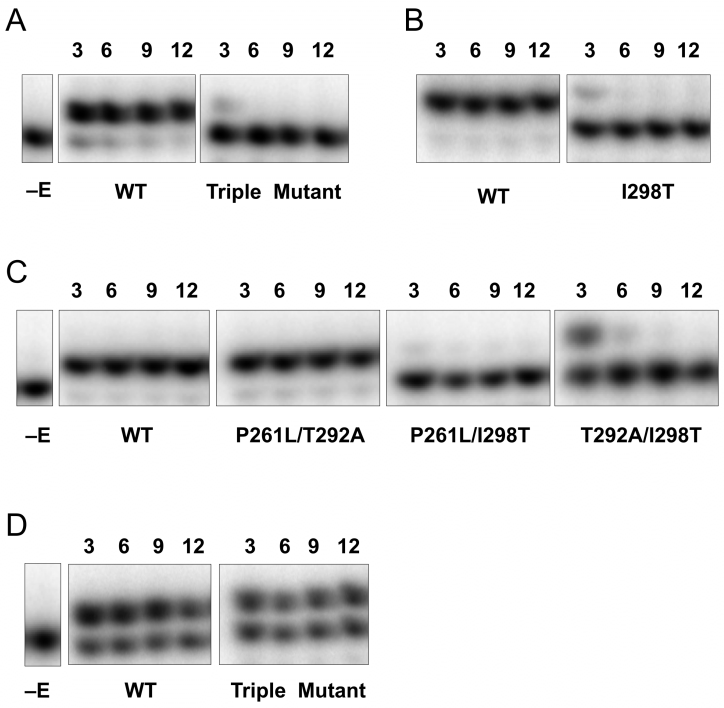
A
3 6 9 12 3 6 9 12
–E
WT
Triple Mutant
B
3 6 9 12 3 6 9 12
WT
I298T
C
3 6 9 12 3 6 9 12 3 6 9 12 3 6 9 12
–E
WT
P261L/T292A
P261L/I298T
T292A/I298T
D
3 6 9 12 3 6 9 12
–E
WT
Triple Mutant

FIGURE 2

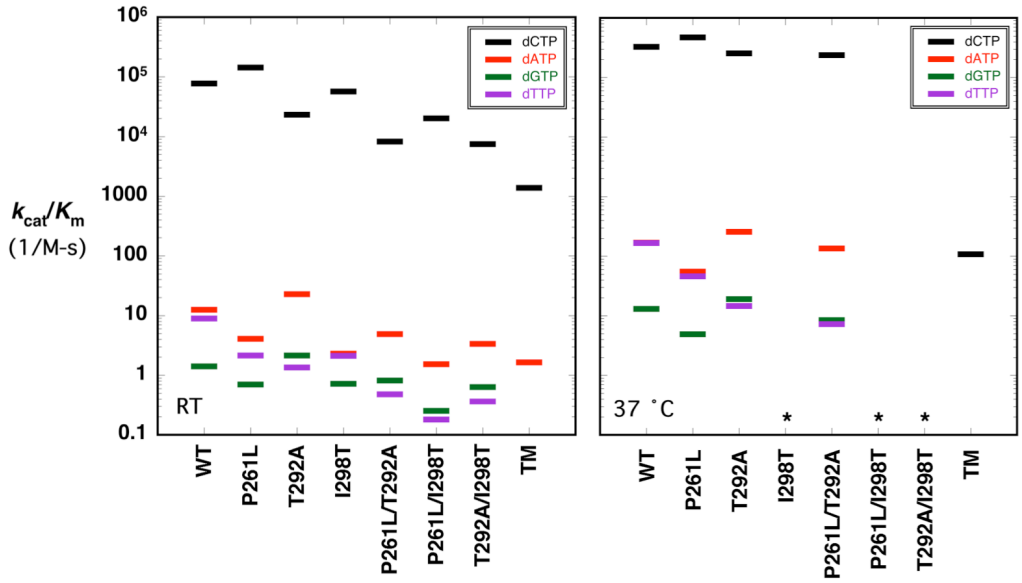
k_{cat}/K_m
(1/M-s)
10^6
10^5
10^4
1000
100
10
1
0.1
dCTP
dATP
dGTP
dTTP
RT
37 ˚C
*
*
*
WT
P261L
T292A
I298T
P261L/T292A
P261L/I298T
T292A/I298T
TM

FIGURE 3

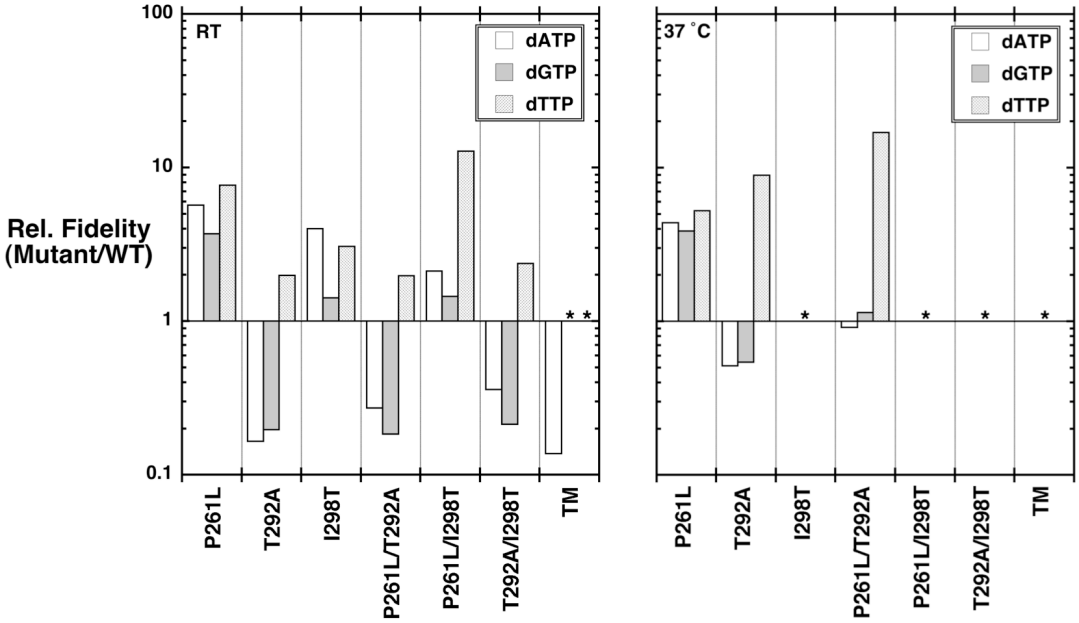
RT
37 ˚C
dATP
dGTP
dTTP
Rel. Fidelity
(Mutant/WT)
100
10
1
0.1
P261L
T292A
I298T
P261L/T292A
P261L/I298T
T292A/I298T
TM

FIGURE 4